

CONSIDERATIONS ON ODR BEAM-SIZE MONITORING FOR GAMMA = 1000 BEAMS*

A.H. Lumpkin, Fermilab, Batavia, IL, U.S.A. 60510

C.-Y. Yao, Argonne National Laboratory, Argonne, IL U.S.A. 60439

E. Chiadroni, M. Castellano, LNF-INFN, Frascati, Italy, A. Cianchi, Univ. of Rome Tor Vergata

Abstract

We discuss the feasibility of monitoring the beam size of $\gamma=1000$ beams with 3000 times more charge in a video frame time and with a more sensitive 12- to 16-bit camera than were used in the previous electron beam studies at 7 GeV at the Advanced Photon Source. Such a beam would be generated at Fermilab in a new facility in the coming years. Numerical integrations of our base model show beam size sensitivity for $\pm 20\%$ level changes at 200- and 400- μm base beam sizes. We also evaluated impact parameters of $5\sigma_y$ and $12\sigma_y$ for both 800-nm and 10- μm observation wavelengths. The latter examples are related to a proposal to apply the technique to an ~ 0.98 TeV proton beam, and this study shows there are trades on photon intensity and beam size sensitivity to be considered at such gammas. In addition, we report on first results at $\gamma=1800$ on a superconducting rf linac.

INTRODUCTION

Characterization of the high-power electron beams of the superconducting rf (SCRF) accelerator to be installed in the New Muon Laboratory (NML) building at Fermilab will be an important aspect of the project [1]. Beam size, position, divergence, emittance, and bunch length measurements are all of interest. Due to the projected high beam power with 3000 micropulses of up to 3 nC each in a macropulse at 5 Hz at eventually up to 1800 MeV, the need for nonintercepting (NI) diagnostics is obvious. Although position is readily addressed with standard rf beam position monitors (BPMs), the transverse size, and hence emittance, are less easily monitored noninterceptively in a linear transport system. Besides an expensive laser-wire system, one of the few viable solutions appears to be the use of optical diffraction radiation (ODR) [2-8] which is emitted when a charged-particle beam passes near a metal-vacuum interface. Appreciable radiation is emitted when the distance of the beam to the screen edge (impact parameter) $b \sim \gamma\lambda/2\pi$, where γ is the Lorentz factor and λ is the observation wavelength. Previous near-field imaging experiments at the Advanced Photon Source (APS) with 7-GeV beams used an impact parameter of 1.25 mm from a single edge of a plane as compared to the scaling factor of ~ 1.4 mm (with an assumed operating wavelength of 0.628 μm) [7]. The near-field images were obtained with a single, 3-nC

micropulse using a standard CCD camera. Since for the NML case, with its much lower gamma, the fields are reduced exponentially as $e^{-2\pi b/\gamma\lambda}$. We either have to use the longer wavelengths in the NIR or FIR or have more charge integrated in the image and a more sensitive camera. The NML design-goal beam intensity gives a factor of 3000, and the intensified or low-noise camera should give another factor of 1000. These two factors combined should allow visible to IR near-field imaging of a beam that is up to 10 to 15 times lower in gamma than the APS case, if similar impact parameters can be used.

We considered focus-at-the-object or near-field imaging optics and established that the perpendicular polarization component of ODR has the beam-size sensitivity that would be needed for a transport line with 400- to 1000- μm rms sizes in the x-plane. These parameters are compatible with the proposed test-area location in the lattice after the SCRF linac [1] as shown in Fig. 1. In addition, we evaluated the possible extension of the technique to a very high intensity hadron beam with $\gamma \sim 1000$ as would be found in the Fermilab Tevatron [2,10]. In the latter application, we also consider a larger impact parameter constraint and the possible compensation of the consequently reduced signal by going to much longer wavelengths. We show there are trades to be considered in this paradigm.

ANALYTICAL BACKGROUND

The basic strategy is to convert the particle-beam information into optical radiation and to take advantage of the power of imaging technology to provide two-dimensional displays of intensity information. These images can be processed for beam size information. Possible radiation sources are optical transition radiation (OTR), ODR, and optical synchrotron radiation (OSR). For completeness, the near-field ODR model as described in Ref. 6 is provided here.

As stated before, ODR is produced when an electron beam passes near a region where different dielectric materials are present. This is generally a vacuum-to-metal interface, and the theory [3-6] is usually for the *far-field* diffraction pattern produced by a beam passing through apertures or slits in conducting planes. In the present case, we effectively integrate over angle and frequency since our optical system is focused on the ODR source itself, i.e. the *near-field* image on the screen. Therefore we proposed a simplified model of the

*Work supported by U.S. Department of Energy, Office of Science, Office of High Energy Physics, under Contract No. DE-AC02-06CH11357.

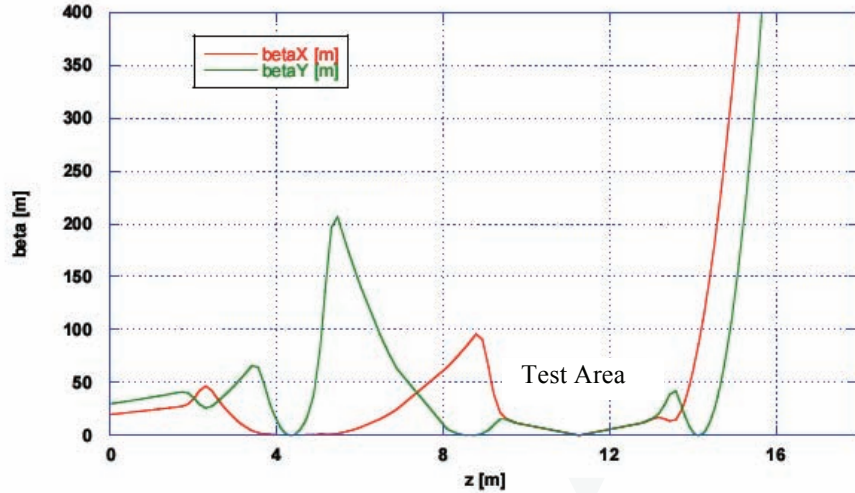


Figure 1: Lattice functions (case 2 waist at $z \sim 11$ m) for the NML Downstream beamline with the proposed three-station configuration indicated by the arrows (lattice plot courtesy of Mike Church, Fermilab).

near field based on the method of virtual quanta described by Jackson [9] in dealing with the photon-like fields of relativistic beams. One convolves the electron beam's Gaussian distribution of sizes σ_x and σ_y with the field expected from a single electron at point P in the metal plane. One wishes to calculate the incoherent sum of radiation from all beam particles in a pulse emitted from a given point on the ODR radiator, i.e. at $\mathbf{u} = \mathbf{P} - \mathbf{r}_0$, where \mathbf{P} is the field point with respect to the origin and \mathbf{r}_0 is the position of the beam centroid with respect to the origin. The impact parameter is $\mathbf{b} = \mathbf{u} - \mathbf{r}$, where $\mathbf{r} = \mathbf{r}(x, y)$ denotes a position in the beam measured from the beam centroid. One then can write the differential spectral intensity as:

$$\frac{dI}{d\omega}(\mathbf{u}, \omega) = \frac{1}{\pi^2} \frac{q^2}{c} \left(\frac{c}{v}\right)^2 \alpha^2 N \frac{1}{\sqrt{2\pi\sigma_x^2}} \frac{1}{\sqrt{2\pi\sigma_y^2}} \times \quad (1)$$

$$\iint dx dy K_1^2(\alpha b) e^{-\frac{x^2}{2\sigma_x^2}} e^{-\frac{y^2}{2\sigma_y^2}}$$

where ω = radiation frequency, v = particle velocity $\approx c$ = speed of light, q = electron charge, N is the particle number, $\alpha = 1/\gamma\lambda$, and $K_1(\alpha b) = K_1\left(\alpha\sqrt{(u_x - x)^2 + (u_y - y)^2}\right)$ is a modified Bessel function. Since one measures light intensity I , this should be proportional to $|E_x|^2 + |E_y|^2$, resulting in the K_1^2 dependence. The incoherent photon intensity is proportional to N , the number of electrons, in contrast to the case of coherent diffraction radiation in the far infrared (FIR), which is enhanced by N^2 .

The APS experiments actually started with a single plane which was inserted vertically. We evaluated the beam size parallel to the single edge. In Fig. 2 we show a calculation of the signal distribution in the optical near field based on this new model for a 7-GeV beam at an

impact parameter of 1250 μm . The beam size was 1375 μm by 200 μm [7].

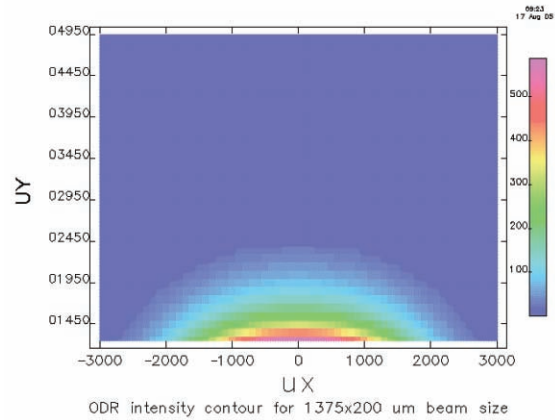


Figure 2: Calculated ODR image for a beam size of 1375 μm by 200 μm and an impact parameter starting at 1250 μm .

NUMERICAL RESULTS

The numerical integrations were done as described previously at PAC07 [11]. In this case the parameters were adjusted to assess the $\gamma=1000$ regime, initially for approximately 500-MeV electrons that are anticipated in the NML at Fermilab. In this case a superconducting linac would be combined with a high-average-current photo injector. Under the scenario of a single semi-infinite metal plane inserted from above the beam axis, we assessed the ODR monitor beam-size sensitivity at a value centered at 200 μm . In Fig. 3 we show both the parallel (p_x) and perpendicular (p_y) components of the ODR profiles for a series of impact parameters. For this beam size near 200 μm and impact parameters, the near-field ODR parallel

component is a two-lobed structure, while the perpendicular component is a single lobe and more directly tracks the beam size. The profile intensities are normalized to one, and it is noted that the vertical profile falls off almost exponentially with impact parameter. The perpendicular polarization component is also 3-4 times more intense than the parallel one.

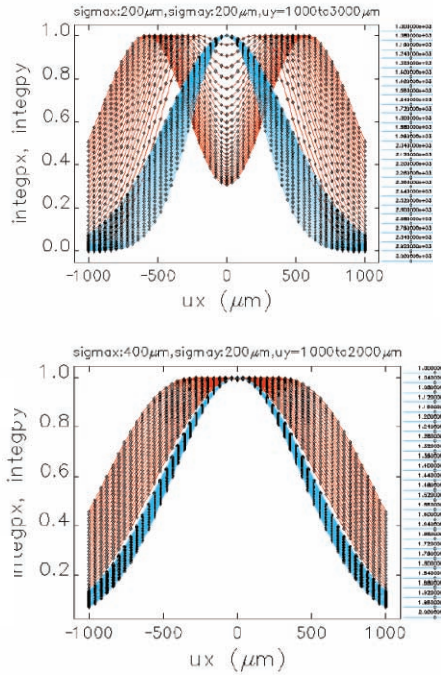


Figure 3: Calculated parallel (red) and perpendicular polarized (blue) ODR profiles for 200 μm (upper) and 400 μm (lower) for impact parameters starting at 1000 μm.

In Fig. 4 we show the ODR perpendicular polarization component for a beam size at 200 μm (upper) and around 400 μm (lower). The observed ODR profile is of course larger than the actual beam size, but the profiles do detectably change in size with the beam size change. A 20% change in beam size from 200 μm, gives ~ 12% change in ODR profile size. We note the calculated ODR profile size is 257 μm for the reference size. We stepped the beam sizes while using fixed input parameters for wavelength of 800 nm and an impact parameter of $5\sigma_y = 1000 \mu\text{m}$.

As an additional issue we addressed the beam size sensitivity for a 400-μm beam size, but with an impact parameter of $12\sigma_y = 5000 \mu\text{m}$ in Fig. 5. Using an 800-nm wavelength, we still calculate some sensitivity to beam size changes of 12 % in the upper plot, but the 10-μm wavelength case shows very little sensitivity in its much larger horizontal profile in the lower plot. A previous proposal [10] had suggested a 14-μm wavelength could be used to increase the photon emission number in an application for protons in the Tevatron using a far-field imaging technique, but the trade is not at all favorable in our near-field technique. So it appears that signal-level permitting, the 800-nm regime would be the better choice as has been used in far-field experiments at 680 MeV by the Frascati team using a 16-bit CCD camera[12].

Transverse profile measurements and diagnostics systems

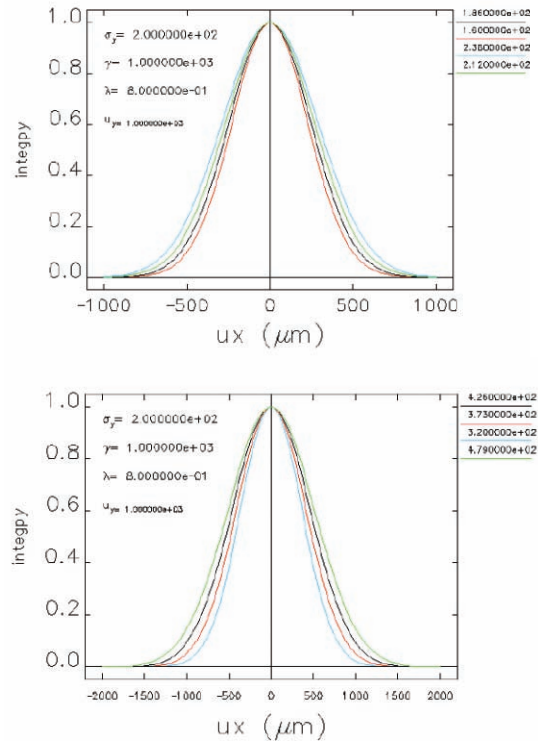


Figure 4: Calculated perpendicular component of horizontal ODR near-field profiles for the variation around 200 μm (upper) and 400 μm (lower).

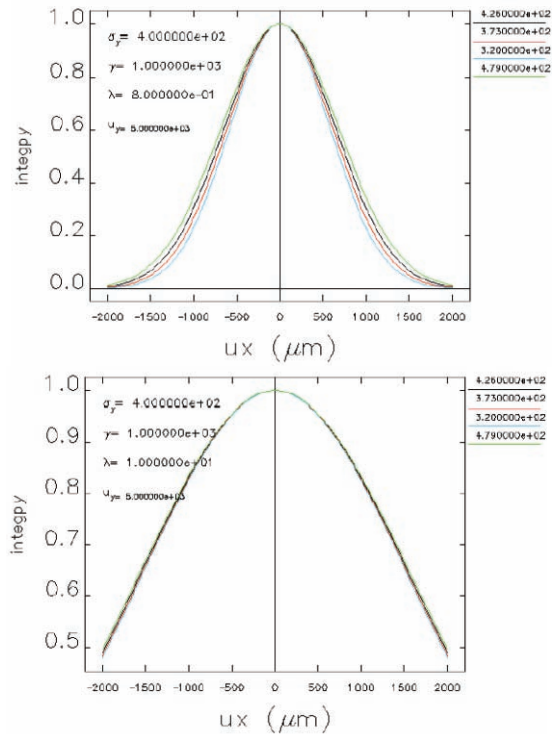


Figure 5: Numerical calculation of the near-field ODR perpendicular component for stepped beam sizes near 400 μm with $b= 5000 \mu\text{m}$, $\gamma=1000$, and $\lambda= 800 \text{ nm}$ (upper) and $\lambda=10 \mu\text{m}$ (lower). The beam-size sensitivity is basically washed out using 10-μm ODR and with this impact parameter of $\sim 12\sigma_y$.

ODR EXPERIMENTAL RESULTS

An opportunity to test the feasibility of the near-field monitor at 900 MeV was identified in discussions with staff at FLASH in Germany and Frascati in Italy. In this case a complementary test was proposed to the ongoing far-field ODR experiments of the Frascati team [12]. The converter consisted of an aluminized Si nitride wafer with a slit chemically etched of 1-mm height. A test beam with 6 bunches and 1 nC per bunch operating at 5 Hz was generated in the FLASH facility and transported to the test station. Ultimately 10 images were summed to improve statistics for the ODR signal obtained using an 800 x 80 nm band pass filter. The beam was positioned on the top edge of the slit, and then the actuator was stepped in 100- μm steps. An example of the image obtained with a 400- μm beam offset from the top edge is shown in Fig. 6. The dark current from the photoinjector has been subtracted from the total beam intensity. The dim ODR image is seen near both top and bottom edges. The ROI sampled only the top image and gave an ODR profile width of about $\sigma_x=360 \mu\text{m}$ as shown in Fig. 7, as compared to the original OTR-measured beam size of 205 μm .

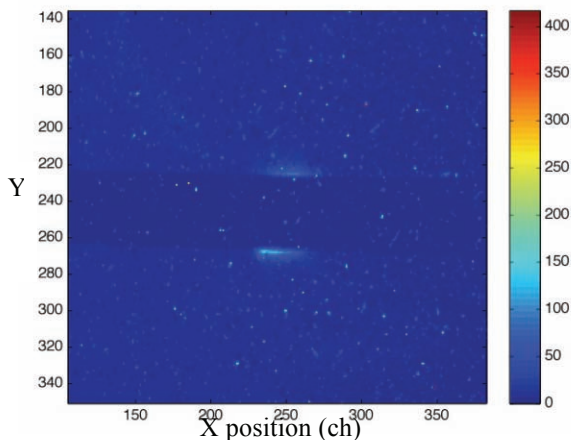


Figure 6: Initial near-field ODR image of the 900-MeV electron beam at FLASH passing through 1-mm tall slit at a location 400 μm below the top edge. This is a 10-image sum with the dark current subtracted from the 16-bit digitized CCD camera data.

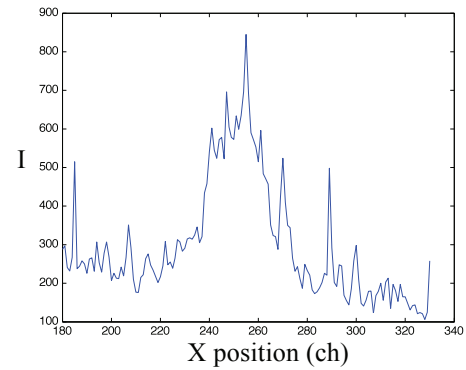


Figure 7: Horizontal profile projection of the ODR top image from Fig. 6. The observed rms width is about 360 μm compared to the OTR image's profile size of 205 μm . The calibration factor is 36.4 μm per channel (ch).

With the first experimental results in the near-field at $\gamma=1800$, we performed post-experiment modeling for these specific parameters. The results of the numerical evaluations are shown in Fig. 8. The top plot shows the total intensity profile for different impact parameters starting at 500 μm . The ODR x profile was calculated to range from 286 μm to 400 μm for impact parameters from 500 to 1200 μm for total intensity, in reasonable agreement with the experiment. The lower plot shows the calculated beam-size sensitivity for the 200 $\mu\text{m} \pm 20\%$ horizontal size. The ODR x-profile clearly tracks the changes with its roughly 30- μm change in sigma per step or 10-12% relative changes. In these cases, the dots on the curves are the ODR results and the solid lines are the Gaussian fits to those points. It is clear the Gaussian assumption is appropriate.

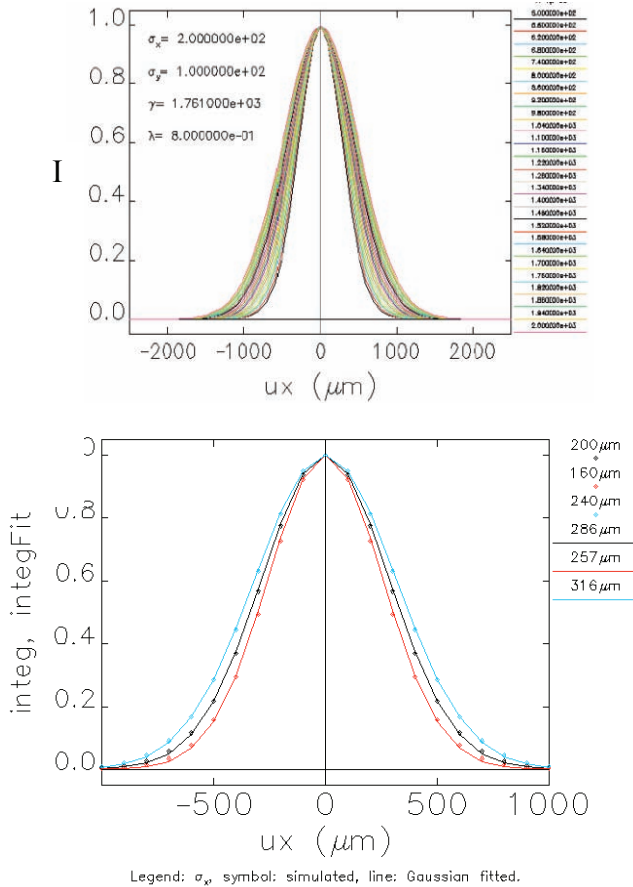


Figure 8: Calculated near-field ODR horizontal profiles for the FLASH case with the variation of impact parameter (top) and the 20% variation of initial beam size around 200 μm (lower).

SUMMARY

In summary, we have extended our investigations on the feasibility of near-field ODR monitoring of particle beams as a noninterceptive method. Our modeling was extended to the challenging $\gamma=1000$ regime to address the potential applications at Fermilab for electrons and possibly protons. With the recent successful proof-of-principle near-field experiment at FLASH at $\gamma\sim 1800$, the scaling to these high-charge, lower gamma beams in the linac now seems more realistic with 800-nm to 1600-nm ODR and an ultra-sensitive CCD camera. The Tevatron proton case is much more difficult due to constraints on the minimum impact parameter allowed and other considerations [13].

ACKNOWLEDGEMENTS

The authors acknowledge support from M. Wendt and S. Nagaitsev of Fermilab and K.-J. Kim of the Argonne Accelerator Institute. We also thank M. Church of Fermilab for the NML lattice calculations and T. Sen for hadron discussions.

REFERENCES

- [1] S. Nagaitsev, ILC-TA Workshop, November 2006, Fermilab.
- [2] Alex H. Lumpkin, "Possible ODR Imaging Diagnostics for ILCTA", presented at ILC-TA Workshop, Fermilab, November 28, 2006.
- [3] M. Castellano, Nucl. Instrum. Methods Phys. Res., A **394**, 275 (1997).
- [4] R. B. Fiorito and D. W. Rule, Nucl. Instrum. Methods Phys. Res. B **173**, 67 (2001).
- [5] T. Muto et al., Phys. Rev. Lett. **90**(10), 104801 (2003).
- [6] P. Karataev et al., Phys. Rev. Lett. **93**, 244802 (2004).
- [7] A.H. Lumpkin, W.J. Berg, N.S. Sereno, D.W. Rule, and C.Y. Yao, Phys. Rev. ST-AB, 10,022802 (2007).
- [8] A.H. Lumpkin et al., "Far-Field OTR and ODR Images Produced by 7-GeV Electron Beams at APS", Proceedings of PAC07, Albuquerque, June 25-29, 2007.
- [9] J.D. Jackson, *Classical Electrodynamics*, (John Wiley and Sons, New York, 1975) Sec. 15.4.
- [10] T. Sen, V. Scarpine, R.Thurman-Keup "Prospects of Diagnostics with ODR in Hadron Colliders", Proc. of PAC07.
- [11] C.-Y. Yao, A.H. Lumpkin, D.W. Rule, "Numerical Simulation of ODR from a 7-GeV Beam", Proc. of PAC07, FRPMS001, Albuquerque, NM.
- [12] E. Chiadroni et al., "Non-Intercepting Electron Beam Transverse Diagnostics with ODR at the DESY FLASH Facility", Proc. of PAC07, Albuquerque, NM.
- [13] Alex H. Lumpkin, "ODR Imaging of Charged Particles: Recent Experiments", presented at the LARP CM10 Meeting, Port Jefferson, NY April 23, 2008.